



Arthrinins A–D: Novel diterpenoids and further constituents from the sponge derived fungus *Arthrinium* sp.

Sherif S. Ebada^{a,h}, Barbara Schulz^b, Victor Wray^c, Frank Totzke^d, Michael H. G. Kubbutat^d, Werner E. G. Müller^e, Alexandra Hamacher^f, Matthias U. Kassack^f, Wenhan Lin^g, Peter Proksch^{a,*}

^a Institut für Pharmazeutische Biologie und Biotechnologie, Heinrich-Heine-Universität, Geb. 26.23, Universitätsstrasse 1, D-40225 Düsseldorf, Germany

^b Institut für Mikrobiologie, Technische Universität Carolo-Wilhelmina zu Braunschweig, Spielmannstrasse 7, D-38106 Braunschweig, Germany

^c Biophysikalische Analytik Abteilung, Helmholtz Zentrum für Infektionsforschung, Inhoffenstrasse 7, D-38124 Braunschweig, Germany

^d ProQinase GmbH, Breisacher Strasse 117, D-79106 Freiburg, Germany

^e Institute for Physiological Chemistry, University Medical Center of the Johannes-Gutenberg-University Mainz, Duesbergweg 6, D-55128 Mainz, Germany

^f Institut für Pharmazeutische und Medizinische Chemie, Heinrich-Heine Universität, Universitätsstrasse 1, Geb. 26.23, D-40225 Düsseldorf, Germany

^g State Key Laboratory of Natural and Biomimetic Drugs, Peking University, Beijing 100083, China

^h Department of Pharmacognosy and Phytochemistry, Faculty of Pharmacy, Ain-Shams University, Organization of African Unity 1, 11566 Cairo, Egypt

ARTICLE INFO

Article history:

Received 21 March 2011

Revised 25 May 2011

Accepted 2 June 2011

Available online 6 July 2011

Dedicated to the memory of Dr. Siegfried Dräger

Keywords:

Diterpenoid

Arthrinium

Cytotoxicity

Protein kinase inhibition

Antiproliferative

ABSTRACT

Bioassay-guided fractionation of a methanolic extract of the fungus *Arthrinium* sp., isolated from the Mediterranean sponge *Geodia cydonium*, afforded 10 natural products including five new diterpenoids, arthrinins A–D (**1–4**) and myrocin D (**5**). In addition, five known compounds were obtained, which included myrocin A (**6**), norlichexanthone (**7**), anomalin A (**8**), decarboxycitrinone (**9**) and 2,5-dimethyl-7-hydroxychromone (**10**). The structures of all isolated compounds were unambiguously elucidated based on extensive 1D and 2D NMR and HR-MS analyzes. The absolute configuration of arthrinins A–D (**1–4**) was established by the convenient Mosher method performed in NMR tubes and by interpretation of the ROESY spectra. Antiproliferative activity of the isolated compounds was assessed in vitro against four different tumor cell lines, including mouse lymphoma (L5178Y), human chronic myelogenous leukemia (K562), human ovarian cancer (A2780) and cisplatin-resistant ovarian cancer cells (A2780CisR), using the MTT assay. Norlichexanthone (**7**) and anomalin A (**8**) exhibited the strongest activities with IC₅₀ values ranging from 0.40 to 74.0 μM depending on the cell line investigated. This was paralleled by the inhibitory activity of both compounds against 16 cancer related protein kinases including aurora-B, PIM1, and VEGF-R2. In vitro IC₅₀ values of **7** and **8** against these three protein kinases ranged from 0.3 to 11.7 μM. Further investigation of the potential antitumoral activity of compounds **5–8** was performed in an in vitro angiogenesis assay against human umbilical vascular endothelial cells (HUVEC) sprouting induced by vascular endothelial growth factor A (VEGF-A). Anomalin A (**8**), myrocin D (**5**) and myrocin A (**6**) inhibited VEGF-A dependent endothelial cell sprouting with IC₅₀ values of 1.8, 2.6 and 3.7 μM, respectively, whereas norlichexanthone (**7**) was inactive.

© 2011 Elsevier Ltd. All rights reserved.

1. Introduction

Marine derived microorganisms such as fungi, bacteria and microalgae have become increasingly important as sources for new bioactive natural products.^{1–5} Marine derived fungi have been shown to be of particular importance as sources of new compounds.^{1,6–27} The first bioactive natural product reported from marine derived fungi dates back to the 1940s when the cephalosporin C producing fungus *Acremonium chrysogenum* was isolated from a sewage outlet in the Mediterranean Sea close to the island of Sardinia. Cephalosporins are still important antibiotics for the

treatment of bacterial infections. Since the discovery of cephalosporin C over 1000 new compounds have been described from fungi that were isolated from various marine sources such as invertebrates (mainly sponges), algae, driftwood or sediment, to name just some of the most frequent sources of fungi that have been mentioned in the literature. Whereas, the importance of marine derived fungi as producers of new bioactive compounds has been amply demonstrated, there is still debate about the true origin of these fungi since many, if not most marine derived fungal strains, belong to ubiquitous genera such as *Aspergillus*, *Penicillium*, *Phoma* and others that are well known from the terrestrial environment.^{1,6,28} It is possible that these fungi even though isolated from marine sources actually originate from terrestrial habitats such as soil from where they are washed into the sea and survive under saline conditions (e.g., as spores in filter feeders such as sponges).

* Corresponding author. Tel.: +49 211 81 14163; fax: +49 211 81 11923.

E-mail address: proksch@uni-duesseldorf.de (P. Proksch).

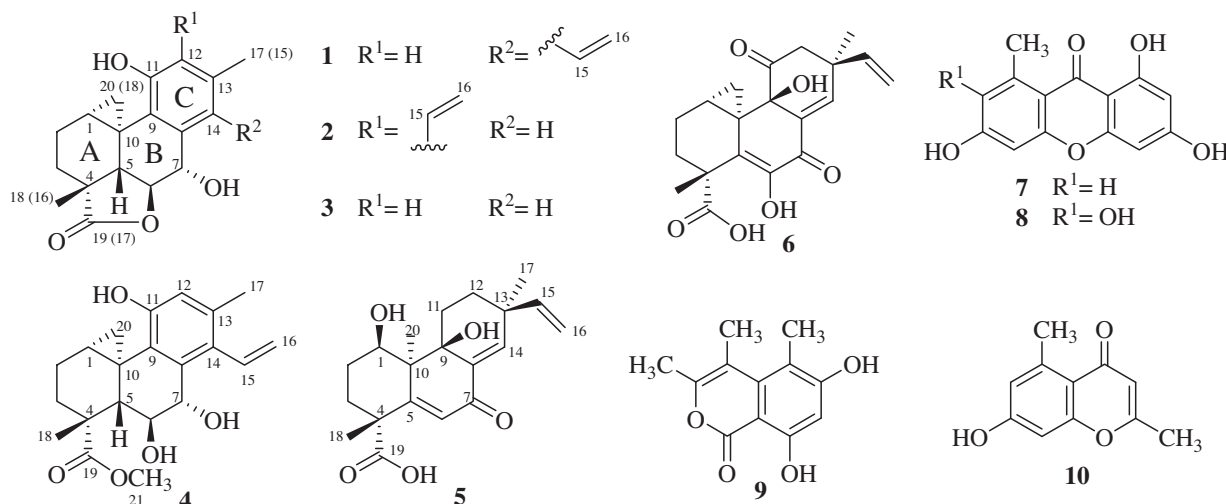


Chart 1.

A terrestrial origin is also quite probable for the sponge derived fungus *Arthrimum* sp. investigated in this study, as members of this genus have been frequently isolated from plant debris and soil in the past. More detailed studies, especially at the molecular level, will be necessary in the future to discriminate between true marine fungal strains and those that may be considered as marine opportunists.

During our continuing research on marine derived fungi, we have now studied *Arthrimum* sp., which was isolated from the internal tissues of the Mediterranean marine sponge *Geodia cydonium* that had been collected in the Adriatic Sea close to Croatia.

Previous chemical investigations of fungal strains of the genus, *Arthrimum*, a dematiaceous anamorph of the teleomorph genus *Apiospora*, revealed a plethora of structurally interesting secondary metabolites such as arthrione,²⁹ arthrichitin,³⁰ terpestacin,³¹ CAF-603,³² norlichexanthone,³³ apiosporamide,³⁴ the cyclopeptides TMC-95A–D,³⁵ and the pimarane-type diterpene myrocin A.³⁶ We now report the isolation and structural elucidation of five new diterpenoids (**1–5**) as well as five known natural products (**6–10**), and on their antiproliferative activities against a panel of human and murine cell lines (Chart 1). For the two most active compounds **7** and **8**, the inhibition of various cancer related protein kinases is shown for the first time.

2. Results and discussion

The methanolic extract of *Arthrimum* sp., isolated from the marine sponge *G. cydonium*, revealed cytotoxic activity against mouse lymphoma (L5178Y) cell line with 99% growth inhibition. Therefore, the total extract was subjected to vacuum liquid chromatography (VLC) on silica gel to purify the active constituents of the extract. Further purification was achieved by preparative HPLC on reversed phase (C-18) to yield five new diterpenoids (**1–5**) together with five known derivatives including myrocin A (**6**),³⁶ norlichexanthone (**7**),³³ anomalin A (**8**),³³ decarboxycitrinone (**9**),³⁷ and 2,5-dimethyl-7-hydroxychromone (**10**).³⁸

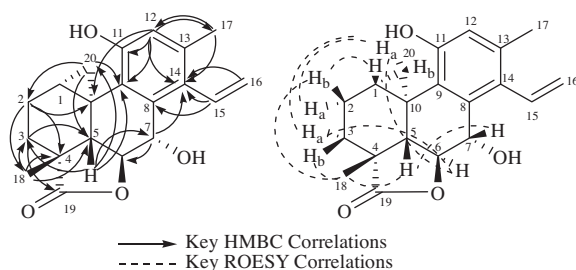
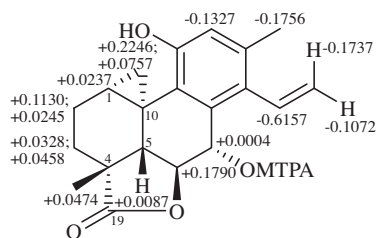
2.1. Novel natural products

The positive and negative ESI-MS of **1** exhibited $[M+H]^+$ and $[M-H]^-$ peaks at m/z 327 and m/z 325, respectively. The molecular formula of **1** was established as $C_{20}H_{22}O_4$ on the basis of its HR-FT-MS $[M+H]^+$ ion peak at m/z 327.1591 implying ten degrees of unsaturation in the molecule. The UV spectrum of **1** revealed absorption bands at λ_{max} 225, 244, and 296 nm suggesting the

presence of an aromatic ring and a γ -lactone ring typical for spruceanol,³⁹ and myrocins B⁴⁰ and C.⁴¹ Inspection of the 1H , ^{13}C NMR and DEPT spectra of **1** (Table 1) revealed 20 carbon signals that account for two methyl, four methylene, six methine, and eight quaternary carbons. 1H and ^{13}C NMR chemical shifts (Table 1) showed the presence of three double bonds and one carbonyl group (δ_C 185.0), and thus the resultant carbon skeleton had to be pentacyclic. Three upfield proton resonances (δ_H 0.66/1.01, H-20, 3.17, H-1) correlated with ^{13}C shifts at δ_C 14.7 (C-20), δ_C 22.1 (C-1) and a ^{13}C signal for a quaternary carbon (C-10) at δ_C 24.6 as shown in the HMQC and HMBC spectra and hence disclosed a cyclopropyl moiety. Also evident from 1H and ^{13}C NMR spectra was an isolated vinyl group (δ_H 5.08/5.37, H-16, 6.92, H-15) which is correlated with ^{13}C shifts at δ_C 117.7 (C-16) and δ_C 138.3 (C-15) as evident from HMQC and HMBC spectra. In addition, H-15 showed correlations to ^{13}C signals at δ_C 134.1, δ_C 135.3, and δ_C 139.8 arising from quaternary carbons C-14, C-13, and C-8, respectively. These correlations conclusively localized the vinyl group at C-14. Based on the inspection of the 1H – 1H COSY spectrum of **1** (Table 1), two main spin systems can be elucidated: one from H-20 to H-2 and the second spin system from H-5 to H-7. In addition, long range correlations between δ_H 6.46/H-12 and δ_H 2.14/CH-17 were observed. In the HMBC spectrum, correlations from H-2 to C-18 and C-19; and from H-3 to C-4 (δ_C 40.5), C-3 (δ_C 23.8), C-5 (δ_C 48.3), and C-19 (δ_C 185.0) were observed that identified the position of the methyl group (CH-18) at C-4. A further HMBC correlation from H-20 to both C-5 and C-10 established the presence of the cyclohexane ring (A). As evident from the 2D NMR data (Table 1), the connection of the cyclopropyl moiety and the cyclohexane ring was confirmed. Strong HMBC correlations (Table 1 and Fig. 1) from H-5 to C-7 (δ_C 75.3), and the quaternary carbon C-9 (δ_C 131.0); from H-7 to the quaternary carbons C-8, C-9, and C-14; from H-20 to C-9; and from H-12 to C-9 confirmed the connection of the aromatic ring (C) to the aliphatic ring (B), which is in turn fused to the cyclohexane ring (A). Based on the 2D ROESY spectrum, the relative configuration of **1** was deduced based on key correlations (Table 1 and Fig. 1) from H-1 to H-2b; from H-20a to H-2a, H-3a, and H-6; from H-5 to H-7 and CH-18; and from CH-18 to H-2b, H-3b, and H-5. In order to determine the absolute configuration of **1**, the modified Mosher procedure⁴² was applied and the observed shift differences between (R)- and (S)- MTPA esters of **1** (Fig. 2) allowed the assignment of the absolute configuration of the chiral center at C-7 as R. This taken together with the results from the ROESY spectrum allowed the determination of the absolute configuration of **1** as 1R, 4R, 5S, 6S,

Table 1
1D and 2D NMR spectral data for **1**

#	δ_H^a (mult., J in Hz)	δ_C^a (mult.)	COSY ^c	HMBC ^{a,d}	ROESY ^b
1	3.17 (m)	22.1 (CH)	2a/b, 20a/b		2a/b
2	2.05 (Hb, td, 3.2, 13.7) 1.84 (Ha, dq, 3.0, 14.0)	21.6 (CH ₂)	2a, 3a/b 2b, 3a/b	3 ^e , 4 ^e	1, 3b, 18 1, 3a/b, 20a ^e
3	1.58 (Ha, td, 3.4, 13.7) 1.42 (Hb, dt, 3.0, 13.9)	23.8 (CH ₂)	2a/b, 3b 2a/b, 3a	2 ^e , 4 ^e , 18 ^e , 19 ^e 2 ^e , 4 ^e , 5 ^e , 18 ^e	2a, 6 ^e , 20a 2a/b, 18
4		40.5 (C)			
5	2.18 (d, 11.9)	48.3 (CH)	6	3, 4, 6, 7, 9, 10, 18, 20	2b, 7, 18
6	4.51 (dd, 7.8, 11.9)	88.2 (CH)	5, 7	5, 7, 10	3a ^e , 20a
7	5.22 (d, 7.8)	75.3 (CH)	6	6, 8, 9, 14	5, 15, 16a
8		139.8 (C)			
9		131.0 (C)			
10		24.6 (C)			
11		152.9 (C)			
12	6.46 (s)	117.6 (CH)	17 ^e	9, 10 ^e , 11, 14, 15 ^e , 17	17
13		135.3 (C)			
14		134.1 (C)			
15	6.92 (dd, 11.2, 18.0)	138.3 (CH)	16a/b	8, 12 ^e , 13, 14	7, 17
16	5.37 (Hb, dd, 2.2, 11.2) 5.08 (Ha, dd, 2.2, 18.0)	117.7 (CH ₂)	15, 16a ^e 15, 16b ^e	14 14, 15	17 ^e 7, 17 ^e
17	2.14 (s)	21.0 (CH ₃)	12 ^e	12, 13, 14, 8 ^e	12, 15, 16a/b ^e
18	1.26 (s)	28.1 (CH ₃)	3a ^e /b ^e	3, 4, 5, 19	2b, 3b, 5
19		185.0 (C)			
20	1.01 (Ha, t, 4.3) 0.66 (Hb, dd, 4.8, 8.5)	14.7 (CH ₂)	1, 20b 1, 20a	2, 5, 9 ^e , 10 ^e 2, 5, 9, 10 ^e	2a ^e , 3a, 6, 20b 20a

^a CD₃OD, 500/125 MHz.^b CD₃OD, 400/100 MHz.^c Assignments are based on extensive 1D and 2D NMR measurements (HMBC, HSQC, COSY).^d Numbers refer to carbon resonances.^e Weak signal.**Figure 1.** Key HMBC and ROESY correlations of arthrinin A (**1**).**Figure 2.** Values of $\delta_S - \delta_R$ of the MTPA esters of arthrinin A (**1**).

7S, 10R. In conclusion, **1** was identified as a new diterpene featuring a hybrid skeleton which is derived from the structural elements of cleistanthane and pimarane diterpenes. It was given the trivial name arthrinin A (**1**).

Compound **2** was isolated as a white amorphous solid. Its ESI-MS revealed the $[M+H]^+$ peak at m/z 327, thus indicating the same molecular weight as that of arthrinin A (**1**). The molecular formula was determined as $C_{20}H_{22}O_4$ on the basis of its HR-FT-MS $[M+Na]^+$ ion peak at m/z 349.1408 which is identical with that of **1**, indicating **2** is an isomer of **1**. This was corroborated by the UV spectrum

of **2** which exhibited absorption bands at λ_{max} 223, 248, and 293 nm and resembled that of arthrinin A (**1**). Comparison of 1H NMR data of **1** (Table 1) and **2** (Table 2) revealed different chemical shifts of the aromatic (δ_H 6.46 in **1** and 6.99 in **2**) and vinyl protons (δ_H 5.08/5.37, H₂-16, and 6.92, H-15 in **1**; and δ_H 5.41/5.59, H₂-16, and 6.60, H-15 in **2**) of both compounds, whereas the remaining signals proved to be identical or very similar. Inspection of the HMBC spectrum of **2** revealed correlations from δ_H 6.99 to C-7 (δ_C 76.9), C-9 (δ_C 131.4), C-12 (δ_C 126.7), and C-17 (δ_C 20.5); from δ_H 5.41/5.59, H₂-16 to C-12; and from δ_H 2.21/CH₃-17 to C-12 and C-13 (δ_C 134.7) which unambiguously located the aromatic proton, vinyl, and methyl functionalities at C-14 (δ_C 124.0), C-12, and C-13, respectively. The relative configuration of **2** was deduced on the basis of a 2D ROESY spectrum which revealed key correlations resembling those exhibited by arthrinin A (**1**). Based on the close structural similarity of the two compounds and their obvious biogenetic relationship, the absolute configuration of **2** was designated as 1R, 4R, 5S, 6S, 7S, 10R. Compound **2** was given the trivial name arthrinin B.

The positive ESI-MS of **3**, which was isolated as a white amorphous solid, revealed the $[M+H]^+$ peak at m/z 301 which is 26 amu smaller than that of arthrinin A (**1**), suggesting the replacement of the vinyl substituents of **1** and **2** by a proton. The molecular formula of **3** was determined by HR-FT-MS, which disclosed $[M+H]^+$ and $[M+Na]^+$ ion peaks at m/z 301.1439 and m/z 323.1256 implying $C_{18}H_{20}O_4$. The absorption bands at λ_{max} 215, 232, and 290 nm in the UV spectrum of **3** suggested the presence of the same chromophore as found in **1** and **2**. A comparison of the 1H and ^{13}C NMR spectra of **3** (Table 2) with those of arthrinins A (**1**) and B (**2**) revealed the absence of proton and carbon resonances originating from the vinyl group and the presence of two meta coupled aromatic protons H-12 and H-14 at δ_H 6.40 and 6.91, respectively. Based on interpretation of the ROESY spectrum and biogenetic considerations, the absolute configuration of **3** was assumed to be identical to that of **1**. Compound **3** was named arthrinin C.

Table 2
¹H and ¹³C NMR spectral data for (2–4)

#	2		3		4	
	δ_H^a (mult., J in Hz)	δ_C^b (mult.)	δ_H^a (mult., J in Hz)	δ_C^b (mult.)	δ_H^a (mult., J in Hz)	δ_C^b (mult.)
1	3.16 (m)	22.6 (CH)	3.11 (m)	22.2 (CH)	2.76 (m)	16.6 (CH)
2	2.05 (Hb, td, 3.2, 13.7)	21.1 (CH ₂)	2.05 (Hb, tt, 3.1, 13.9)	21.0 (CH ₂)	2.10 (Hb, m)	21.8 (CH ₂)
	1.84 (Ha, dq, 3.0, 14.0)		1.83 (Ha, dq, 3.0, 14.1)		1.64 (Ha, m)	
3	1.60 (Ha, td, 3.2, 13.7)	24.0 (CH ₂)	1.59 (Ha, td, 3.6, 13.7)	24.1 (CH ₂)	1.92 (Ha, m)	34.1 (CH ₂)
	1.45 (Hb, dt, 3.0, 14.0)		1.44 (Hb, dt, 3.1, 13.9)		1.28 (Hb, m)	
4		40.3 (C)		40.2 (C)		44.6 (C)
5	2.27 (d, 11.4)	48.6 (CH)	2.25 (d, 11.5)	48.2 (CH)	1.77 (d, 8.4)	54.8 (CH)
6	4.42 (dd, 8.7, 11.4)	86.8 (CH)	4.41 (dd, 8.8, 11.4)	87.0 (CH)	4.73 (dd, 2.0, 8.4)	76.6 (CH)
7	4.95 (d, 8.7)	76.9 (CH)	4.93 (d, 9.1)	77.1 (CH)	4.96 (d, 2.0)	77.0 (CH)
8		140.4 (C)		141.9 (C)		139.3 (C)
9		131.4 (C)		129.8 (C)		130.1 (C)
10		24.9 (C)		24.7 (C)		21.7 (C)
11		150.3 (C)		153.9 (C)		152.9 (C)
12		126.7 (C)	6.40 (br s)	116.5 (CH)	6.51 (s)	118.7 (CH)
13		134.7 (C)		136.9 (C)		132.6 (C)
14	6.99 (s)	124.0 (CH)	6.91 (br s)	122.5 (CH)		135.4 (C)
15	6.60 (dd, 11.5, 18.0)	132.9 (CH)	2.20 (s)	21.1 (CH ₃)	6.77 (dd, 11.4, 17.9)	136.0 (CH)
16	5.59 (Hb, dd, 1.9, 11.5)	121.5 (CH ₂)	1.28 (s)	28.6 (CH ₃)	5.45 (Hb, dd, 2.0, 11.4)	119.4 (CH ₂)
	5.41 (Ha, dd, 1.9, 18.0)				5.32 (Ha, dd, 2.0, 17.9)	
17	2.21 (s)	20.5 (CH ₃)		185.0 (C)	2.15 (s)	20.7 (CH ₃)
18	1.29 (s)	28.5 (CH ₃)	0.99 (Ha, t, 4.3)	15.2 (CH ₂)	1.31 (s)	29.0 (CH ₃)
			0.56 (Hb, dd, 4.7, 8.5)			
19		184.9 (C)				179.3 (C)
20	1.01 (Ha, t, 4.3)	15.4 (CH ₂)			0.87 (Ha, t, 5.1)	19.3 (CH ₂)
	0.60 (Hb, dd, 4.7, 8.6)				0.52 (Hb, dd, 4.7, 9.3)	
21-OMe					3.66 (s)	52.1 (CH ₃)

^a CD₃OD, 500/125 MHz.^b CD₃OD, 400/100 MHz.

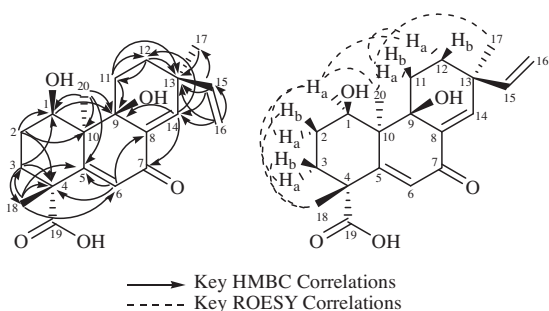
The molecular formula of **4** was determined as C₂₁H₂₆O₅ by HR-FT-MS which exhibited a [M+Na]⁺ peak at *m/z* 381.1666, and which is 32 atomic mass units larger than that of arthrinins A (**1**) and B (**2**). The UV spectrum of **4** revealed four absorption bands at λ_{\max} 210, 235, 263, and 320 nm and differed from those of arthrinins A–C (**1–3**), which displayed only three bands. This suggested a modified skeleton for **4**. ¹H, ¹³C NMR, and DEPT spectra (Table 2), when compared to those of arthrinin A (**1**), displayed one additional methyl resonance at δ_H 3.66, which was an oxygen-substituted singlet and correlated to the ¹³C resonance at δ_C 52.1 ppm, suggesting the existence of a methyl ester functionality in the molecule. Inspection of the HMBC spectrum of **4** showed key correlations from the aromatic and vinyl protons similar to those of arthrinin A (**1**), indicating the position of the aromatic proton and the vinyl group at C-12 and C-14, respectively. Moreover, the HMBC spectrum of **4** revealed a strong correlation from the methyl groups at δ_H 1.31/CH₃-18 and δ_H 3.66 with C-19 (δ_C 179.3), suggesting the presence of a methyl ester group at C-19 and an opened γ -lactone ring. ROESY spectrum of **4** exhibited key correlations from H-1 to H-2b; from H-20a to H-3a and H-6; from H-5 to H-3b, and H-7; and from H₃-18 to H-3b, implying the same relative configuration of **4** as previously observed for **1–3**. Compound **4** was named arthrinin D.

The ESI-MS of **5** displayed [M+H]⁺ and [M–H][–] peaks at *m/z* 347 and *m/z* 345, respectively. The molecular formula of **5** was determined to be C₂₀H₂₆O₅ based on its HR-FT-MS [M+H]⁺ peak at *m/z* 347.1849 implying eight degrees of unsaturation. The ¹³C and DEPT spectra of **5** (Table 3) indicated the presence of 20 carbon signals, including three methyl, five methylene, four methine, and eight quaternary carbons including two carbonyl carbons. Considering the molecular formula of **5**, the three remaining protons had to be present as hydroxyl groups. The UV spectrum of **5** displayed three absorption bands at λ_{\max} 219, 273, and 310 nm, thus differing from that of arthrinins A–D (**1–4**). Inspection of ¹H and ¹³C NMR data of **5** (Table 3) and comparison with data reported in the liter-

ature suggested a pimarane diterpene skeleton similar to that present in myrocins A–C^{36,40,41} as the core structure of **5**. However, the absence of the three upfield proton resonances (δ_H 0.83/1.13, H₂-20, 1.85, H-1) that are present in the ¹H NMR spectrum of myrocin A (**6**) and the existence of an additional methyl group at δ_H 1.21 and proton signal at δ_H 4.35 (dd, *J* = 4.4, 10.6 Hz) in the ¹H NMR spectrum of **5** indicated that the cyclopropyl ring was absent and had been replaced by a methyl group at C-10 and a hydroxyl group at C-1. Moreover, inspection of the ¹H NMR spectral data of **5** (Table 3) showed the presence of two olefinic protons at δ_H 5.26/H-6 and δ_H 6.86/H-14 both conjugated to a ketone (δ_C 180.4) and of an isolated vinyl group (δ_H 5.05/5.10, H₂-16, 5.90, H-15). Structural elucidation of **5** was further confirmed by 2D NMR spectroscopy (Table 3 and Fig. 3) including ¹H–¹H COSY, HMBC, HMQC, and ROESY. ¹H–¹H COSY spectrum of **5** revealed the presence of two spin systems from H-1 to H₂-3 and between H₂-11 and H₂-12 with the latter extending to the olefinic proton H-14. In the HMBC spectrum of **5** (Fig. 3), key correlations were identified from H₂-3 to C-18 and from H₃-18 to the quaternary carbon C-4, proving that the methyl group (CH₃-18) was located at C-4 (δ_C 49.8). In addition H₃-18 correlated with the sp²-hybridized carbons C-5 (δ_C 147.4) and C-6 (δ_C 109.1), and thus C-5 was located between C-4 and C-6. HMBC correlations from the methyl group at δ_H 1.21/CH₃-20 to C-5, C-10 (δ_C 48.6), and to the oxygenated quaternary carbon C-9 (δ_C 76.5) located the methyl substituent CH₃-20 at C-10. Moreover, the ¹H–¹H COSY correlations observed between H-15 and H₂-16 established that, as deduced from HMBC correlations (Fig. 3), in addition to a singlet methyl group (δ_H 1.14/CH₃-17) a vinyl group was also bound to the quaternary carbon C-13 (δ_C 39.3). Also evident in the HMBC spectrum of **5** were correlations from the olefinic proton H-14 (δ_H 6.86) to C-9, C-12 (δ_C 31.1), C-13, and to the carbonyl C-7 (δ_C 180.4), confirming the presence of the α,β -unsaturated ketone. The relative configuration of **5** was determined on the basis of the ROESY spectrum which revealed diagnostic correlations (Table 3 and Fig. 3) from H-1 to H-2a, H-3a, and H-12a; from

Table 3
1D and 2D NMR spectral data of **5**

#	$\delta_{\text{H}}^{\text{a}}$ (mult., J in Hz)	$\delta_{\text{C}}^{\text{b}}$ (mult.)	COSY ^c	HMBC ^{a,d}	ROESY ^b
1	4.35 (dd, 4.4, 10.6)	70.0 (CH)	2a/b, 3a ^e /b ^e	2, 9, 20	2a/b, 3a/b ^e , 11b ^e , 12a, 20 ^e
2	1.93 (Hb, m)	29.2 (CH ₂)	1, 2a, 3a/b	1 ^e , 3 ^e , 10 ^e , 18	1, 2a, 18
	1.80 (Ha, m)		1, 2b, 3a/b	1 ^e , 3, 10 ^e	1, 2b
3	1.92 (Ha, m)	27.5 (CH ₂)	1, 2a/b, 3b	1 ^e , 4, 5 ^e	1, 3b, 20
	1.50 (Hb, td, 3.0, 15.0)		1, 2a/b, 3a	1 ^e , 4 ^e , 5 ^e , 18	1 ^e , 3a
4		49.8 (C)			
5		147.4 (C)			
6	5.26 (s)	109.1 (CH)		4, 5, 8, 18	3a ^e /b ^e , 18 ^e
7		180.4 (C)			
8		138.3 (C)			
9		76.5 (C)			
10		48.6 (C)			
11	2.30 (Ha, td, 3.4, 14.4)	29.1 (CH ₂)	11b, 12a/b	12, 13	11b, 12a/b, 17, 20
	2.05 (Hb, dt, 4.0, 14.8)		11a, 12a/b	8, 9, 12, 13 ^e	1 ^e , 11a, 12a/b
12	1.85 (Ha, m)	31.1 (CH ₂)	11a/b, 12b	11 ^e , 13 ^e	1, 11a/b, 12b, 15 ^e , 20
	1.50 (Hb, td, 3.0, 15.0)		11a/b, 12a, 14	11 ^e , 13 ^e	1 ^e , 11a/b, 12a
13		39.3 (C)			
14	6.86 (d, 1.0)	147.6 (CH)	12b	7, 8, 9, 12, 13, 15	15 ^e , 16a ^e , 17 ^e
15	5.90 (dd, 10.7, 17.5)	147.3 (CH)	16a/b	12, 13, 14, 17	12a ^e , 17 ^e
16	5.05 (Ha, d, 10.7)	112.8 (CH ₂)	15	13, 15	
	5.10 (Hb, d, 17.5)		15	13, 15	12a ^e /b ^e , 17 ^e
17	1.14 (s)	24.0 (CH ₃)		12, 13, 14, 15, 16 ^e	11a, 12b ^e , 14 ^e , 15, 16a ^e /b ^e
18	1.31 (s)	25.5 (CH ₃)		3, 4, 5, 6	2b, 3b ^e , 6 ^e
19		180.4 (C)			
20	1.21 (s)	18.1 (CH ₃)		1, 5, 9, 10	1 ^e , 11a, 3a

^a CD₃OD, 500/125 MHz.^b CD₃OD, 400/100 MHz.^c Assignments are based on extensive 1D and 2D NMR measurements (HMBC, HSQC, COSY).^d Numbers refer to carbon resonances.^e Weak signal.**Figure 3.** Key HMBC and ROESY correlations of myrocin D (**5**).

methyl group (CH₃-18) to H-2b, and H-3b; from methyl group (CH₃-17) to H-11a; and from methyl group (CH₃-20) to H-11a, and H-3a, clearly positioning the two methyl groups (CH₃-17 and CH₃-20) on the same side of the molecule unlike methyl group (CH₃-18), positioned on the opposite face. Except for C-1, the relative configuration of **5** was in agreement with that previously reported for the pimarane diterpene derivative, myrocin A (**6**).³⁶ We propose the trivial name myrocin D for **5**.

2.2. Bioactivity

All isolated compounds were tested *in vitro* for their antiproliferative activity against four different tumor cell lines including mouse lymphoma (L5178Y), human chronic myelogenous leukemia (K562), human ovarian cancer (A2780) and cisplatin-resistant human ovarian cancer cells (A2780CisR) by using the MTT assay with kahalalide F or cisplatin (CDDP) as positive controls. Results of the MTT assay (Table 4) revealed that of the tested diterpenoids, only myrocins D (**5**) and A (**6**) revealed antiproliferative activities, in contrast to the arthrinins A–D (**1–4**), which were inactive. Thus, it seems that the pimarane diterpene skeleton is essential for cytotoxicity. Anomalin A (**8**) exhibited significant and selective

Table 4
IC₅₀ values of selected compounds against four different tumor cell lines

Compound	IC ₅₀ (μM)			
	L5178Y	K562	A2780	A2780CisR
Myrocin D (5)	2.05	50.3	41.3	66.0
Myrocin A (6)	2.74	42.0	28.2	154.7
Norlichexanthone (7)	1.16	253.50	68.2	74.0
Anomalin A (8)	0.40	n.a.	4.34	26.0
Kahalalide F (positive control)	4.30	—	—	—
Cisplatin (CDDP) (positive control)	—	7.80	0.80	8.40

n.a.: not active up to 365 μM.

antiproliferative activities compared to its deoxy derivative, norlichexanthone (**7**). Interestingly, anomalin A (**8**) revealed IC₅₀ values of 0.40, 4.34, and 26.0 μM against L5178Y, A2780, and A2780CisR tumor cell lines, respectively. However, it was not active against the human chronic myelogenous leukemia (K562) cell line.

To further investigate possible mechanisms of action of the active compounds (**5–8**), they were assayed *in vitro* for their protein kinase inhibitory activity at 1 and 10 μM concentrations against 16 different protein kinases. Among the tested compounds, 1 μM concentration of both norlichexanthone (**7**) and anomalin A (**8**) inhibited one or more of the tested kinases by at least 40%. Hence, the IC₅₀ values of **7** and **8** against all 16 protein kinases (Table 5) were determined. Compounds **7** and **8** inhibited protein kinases ALK, ARK5, Aurora-B, IGF1-R, PIM1, PLK1, PRK1, SRC, and VEGF-R2 with IC₅₀ values between 0.3 and 75.7 μM. Unlike norlichexanthone (**7**), anomalin A (**8**) showed detectable inhibitory activities against AXL, FAK, and MET wt with IC₅₀ values of 6.6, 15.2, and 4.4 μM, respectively. Conclusively, the parallel pattern of cytotoxicity and protein kinase inhibitory activity of norlichexanthone (**7**) and anomalin A (**8**) suggests that inhibition of protein kinases may be one of the major mechanisms contributing to their antiproliferative activity.

Further investigation of the mechanism of action of compounds (**5–8**) was performed through conducting the *in vitro* angiogenesis

Table 5IC₅₀ values of selected compounds against 16 different protein kinases^a

Compound	AKT1	ALK	ARK5	Aurora-B	AXL	FAK	IGF1-R	MEK1 wt
Norlichexanthone (7)	n.a.	41.3	33.0	3.0	n.a.	n.a.	33.3	n.a.
Anomalin A (8)	n.a.	1.1	15.6	0.5	6.6	15.2	8.6	n.a.
Compound	MET wt	NEK2	NEK6	PIM1	PLK1	PRK1	SRC	VEGF-R2
Norlichexanthone (7)	n.a.	n.a.	n.a.	0.3	75.7	54.9	35.0	11.7
Anomalin A (8)	4.4	83.9	67.8	0.3	8.8	45.3	12.9	0.8

^a Inhibitory potentials of compounds at various concentrations were determined in biochemical protein kinase activity assays. Listed are IC₅₀ values in μM . n.a.: not active, i.e., IC₅₀ > 100 μM .

Table 6IC₅₀ values of selected compounds for the inhibition of VEGF-A induced endothelial cell sprouting in a cellular angiogenesis assay

Compound	IC ₅₀ (μM)
Myrocin D (5)	2.60
Myrocin A (6)	3.70
Norlichexanthone (7)	n.c.
Anomalin A (8)	1.80
Sunitinib (positive control)	0.12

n.c.: no change.

assay against human umbilical vascular endothelial cells (HUVEC) sprouting induced by vascular endothelial growth factor A (VEGF-A) using sunitinib as a positive control. Results (Table 6) revealed that anomalin A (8) inhibited VEGF-A dependent endothelial cells sprouting with IC₅₀ value of 1.8 μM corresponding to its in vitro inhibitory activity against VEGF-R2 protein kinase (IC₅₀ = 0.8 μM). Norlichexanthone (7) showed no effect in the angiogenesis assay in spite of inhibiting VEGF-R2 protein kinase with IC₅₀ values of 11.7 μM . However, whereas myrocins D (5) and A (6) were inactive in the protein kinase inhibitory activity assay, they revealed significant activities in the angiogenesis assay with IC₅₀ values of 2.6 and 3.7 μM , respectively, compared to sunitinib (IC₅₀ = 0.12 μM). This discrepancy can perhaps be explained by the intracellular modification of 5 and 6 into active metabolites which were not present in the protein kinase inhibitory activity assay.

3. Experimental section

3.1. General experimental procedures

Optical rotation was recorded using a Perkin–Elmer-241 MC polarimeter. ESI-MS were obtained on a ThermoFinnigan LCQ DECA mass spectrometer coupled to an Agilent 1100 HPLC system equipped with a photodiode array detector. HR-FT-MS was recorded on a LTQ FT-MS-Orbitrap (ThermoFinnigan, Bremen, Germany). 1D and 2D NMR spectra were recorded at 300 K on either Bruker ARX-400 or Bruker ARX-500 NMR spectrometer locked to the major deuterium resonance of the solvent, CD₃OD.

For analytical HPLC analysis, samples were injected into a HPLC system equipped with a photodiode array detector (Dionex, Munich, Germany). Routine detection was at 235, 254, 280, and 340 nm. The separation column (125 × 4 mm ID) was prefilled with C-18 Euro-sphere, 5 μM (Knauer, Berlin, Germany). Separation was achieved by applying a linear gradient from 90% H₂O (pH 2.0) to 100% MeOH over 40 min. TLC analysis was carried out using aluminium sheet precoated with silica gel 60 F₂₅₄ (Merck, Darmstadt, Germany).

Preparative HPLC separations were performed on a LaChrom–Merck Hitachi HPLC system, pump L-7100, UV detector L-7400 using a C-18 column (Knauer, 300 × 8 mm ID, prefilled with C-18 Euro-sphere, flow rate 5 mL/min, UV detection at 280 nm); the solvent system consisted of a linear gradient of MeOH and nanopure H₂O.

3.2. Isolation and cultivation of the fungus

The sponge *G. cydonium*, collected from the Adriatic Ocean near Italy, was subjected to a partial surface sterilization by immersing in 70% ethanol for 30 s. followed by rinsing three times in sterilized artificial sea water. Then, the sponge was cleaved aseptically into small segments ($\approx 1.5 \times 1.5$ mm). The material was placed on a potato carrot agar medium²⁸ and incubated at room temperature (≈ 21 °C). After several days, hyphae growing from the sponge material were transferred to fresh plates with the same medium, incubated again and periodically checked for culture purity. The fungus (internal strain no. 9287) was identified as *Arthrimum* sp. (Sordariomycetes) by morphological characterization on the basis of the description in Ellis (1971).⁴³ Large scale growth of the fungus, for the isolation and identification of secondary metabolites, was carried out on a barley–spelt medium (200 g barley, 200 g spelt, 2 g soy protein, 2 mg MnCl₂ und 250 mL distilled water) at room temperature for 28 days at ≈ 22 °C.

3.3. Extraction and isolation

The bioactive methanolic extract was evaporated under reduced pressure to yield 7.0 g residue. This residue was subjected to vacuum liquid chromatography (VLC) on a silica gel column employing a step gradient of *n*-hexane–EtOAc and then CH₂Cl₂–methanol yielding 14 fractions each of 500 mL. These fractions were dried and examined by TLC on premade silica gel plates (Merck, Darmstadt, Germany) using a dichloromethane–methanol based solvent system.

Further purification of the fractions obtained with 75% and 25% *n*-hexane in EtOAc, and 90% and 80% dichloromethane in methanol was achieved by semi-preparative reversed phase HPLC to yield **1** (14.0 mg), **2** (2.0 mg), **3** (2.6 mg), **4** (2.0 mg), **5** (12.5 mg), **6** (15.3 mg), **7** (26.0 mg), **8** (95.8 mg), **9** (1.0 mg), **10** (3.3 mg).

3.3.1. Arthrinin A (1)

White amorphous solid; $[\alpha]_D^{22} +130.6$ (*c* 1.40, MeOH); UV (MeOH) λ_{max} 225, 244, 296 nm; ¹H NMR (methanol-*d*₄, 500 MHz) and ¹³C NMR (methanol-*d*₄, 125 MHz), 2D NMR data, see Table 1; HR-FT-MS *m/z* 327.1591 [M+H]⁺ (calcd for C₂₀H₂₃O₄, 327.1596).

3.3.2. Arthrinin B (2)

White amorphous solid; $[\alpha]_D^{22} +48.0$ (*c* 0.20, MeOH); UV (MeOH) λ_{max} 223, 248, 293 nm; ¹H NMR (methanol-*d*₄, 500 MHz) and ¹³C NMR (methanol-*d*₄, 100 MHz) data, see Table 2; HR-FT-MS *m/z* 349.1408 [M+Na]⁺ (calcd for C₂₀H₂₂O₄Na, 349.1410).

3.3.3. Arthrinin C (3)

White amorphous solid; $[\alpha]_D^{22} +62.0$ (*c* 0.26, MeOH); UV (MeOH) λ_{max} 215, 232, 290 nm; ¹H NMR (methanol-*d*₄, 500 MHz) and ¹³C NMR (methanol-*d*₄, 100 MHz) data, see Table 2; HR-FT-MS *m/z* 301.1439 [M+H]⁺ (calcd for C₁₈H₂₁O₄, 301.1434), *m/z* 323.1256 [M+Na]⁺ (calcd for C₁₈H₂₀O₄Na, 323.1254).

3.3.4. Arthrinin D (4)

White amorphous solid; $[\alpha]_D^{22} +18.0$ (c 0.20, MeOH); UV (MeOH) λ_{\max} 210, 235, 263, 320 nm; ^1H NMR (methanol- d_4 , 500 MHz) and ^{13}C NMR (methanol- d_4 , 100 MHz) data, see Table 2; HR-FT-MS m/z 381.1666 $[\text{M}+\text{Na}]^+$ (calcd for $\text{C}_{21}\text{H}_{26}\text{O}_5\text{Na}$, 381.1672).

3.3.5. Myrocin D (5)

Yellow powder; $[\alpha]_D^{22} +18.2$ (c 1.25, MeOH); UV (MeOH) λ_{\max} 219, 273, 310 nm; ^1H NMR (methanol- d_4 , 500 MHz) and ^{13}C NMR (methanol- d_4 , 125 MHz), 2D NMR data, see Table 3; HR-FT-MS m/z 347.1849 $[\text{M}+\text{H}]^+$ (calcd for $\text{C}_{20}\text{H}_{27}\text{O}_5$, 347.1853), m/z 369.1667 $[\text{M}+\text{H}]^+$ (calcd for $\text{C}_{20}\text{H}_{26}\text{O}_5\text{Na}$, 369.1672).

3.4. Cell proliferation assay

Antiproliferative activity was tested in vitro against mouse lymphoma (L5178Y), human chronic myelogenous leukemia (K562), human ovarian cancer (A2780) and cisplatin-resistant human ovarian cancer cells (A2780CisR) cell lines using a microplate based 3-(4,5-dimethylthiazol-2-yl)-2,5-diphenyltetrazolium bromide (MTT) assay and compared to that of untreated controls as previously described.^{44,45} All experiments were carried out in triplicate. The depsipeptide kahalalide F or cisplatin (CDDP) were used as positive controls.

3.5. Assay for inhibition of protein kinase

An assay for inhibition of protein kinase was conducted in vitro as previously described.⁴⁶ In brief, all biochemical protein kinase activity assays were performed in 96-well FlashPlates from Perkin-Elmer/NEN (Boston, MA) in a 50 μL reaction volume. The reaction mixture contained 20 μL of assay buffer, 5 μL of ATP solution (in H_2O), 5 μL of test compound (in 10% DMSO), 10 μL of substrate, and 10 μL of purified recombinant protein kinase. The assay for all enzymes contained 70 mM HEPES–NaOH, pH 7.5, 3 mM MgCl_2 , 3 mM MnCl_2 , 3 μM Na-orthovanadate, 1.2 mM DDT, 50 $\mu\text{g}/\text{mL}$ PEG₂₀₀₀₀, and 1 μM $[\gamma\text{-}^{33}\text{P}]\text{-ATP}$ (ca. 8×10^5 cpm per well). The following substrates were used: GSK3(14–27), AKT1, NEK6, PIM1; RBER-CHKtide, PLK1, PRK1, ARK5; tetra(LRRWSLG), Aurora-B; ERK2-KR, MEK1 wt; poly(Ala, Glu, Lys, Tyr)_{6:2:5:1}, MET wt; RB-CTF, NEK2; poly(Glu, Tyr)_{4:1}, ALK, FAK, IGF1-R, SRC, VEGF-R2, AXL. The reaction mixtures were incubated at 30 °C for 60 min. The reaction was stopped with 50 μL of 2% (v/v) H_3PO_4 ; plates were then aspirated and washed twice with 200 μL of 0.9% (w/v) NaCl. Incorporation of ^{33}P was determined with a microtiter scintillation counter (Microbeta, Wallac). All assays were performed with a BeckmanCoulter/SAGIANTM Core System. IC₅₀ values were assayed for those compounds possessing at least 40% inhibitory activity against one of the tested protein kinases. To determine IC₅₀ values, 10 concentrations (100 μM to 3 nM) of each compound were tested in singlicate. Then, the residual activities for each concentration and the IC₅₀ values were calculated using Quattro Workflow V3.0.6 (Quattro Research GmbH, Munich, Germany).

3.6. Angiogenesis assay

The assay was pursued in modification of the originally published protocol.⁴⁷ In brief, spheroids were prepared as previously described⁴⁸ by pipetting 500 HUVEC in a hanging drop on plastic dishes to allow overnight spheroid aggregation. Fifty HUVEC spheroids were then seeded in 0.9 mL of a collagen gel and pipetted into individual wells of a 24 well plate to allow polymerization. The test compounds in combination with VEGF-A [25 ng/mL final assay concentration] were added after 30 min by pipetting 100 μL of a 10-fold concentrated working dilution on top of the polymerized

gel. Plates were incubated at 37 °C for 24 h and fixed by adding 4% paraformaldehyde.

Sprouting intensity of HUVEC spheroids treated with the test compounds were scanned under the microscope by two independent observers for changes compared to VEGF-A control and documented. Sprouting intensity of HUVEC spheroids treated with the identified inhibitors and stimulators or sunitinib were quantified by an image analysis system determining the cumulative sprout length per spheroid using an inverted microscope and the digital imaging software Analysis 3.2 (Soft imaging system, Münster, Germany). The mean of the cumulative sprout length of 10 randomly selected spheroids was analyzed as an individual data point. To determine IC₅₀ values, seven concentrations (10 μM to 10 nM) of each compound were tested in singlicate and the calculations were performed using GraphPad Prism version 5.02 software.

3.7. Chiral derivatization

The reaction was conducted according to the Mosher ester procedure as described by Kinghorn and co-workers.⁴² In brief, the compound (2 \times 2.0 mg) was transferred into clean dry NMR tubes and dried under vacuum. The samples were dissolved in deuterated pyridine (0.75 mL), and 10 μL of (R)- and (S)-MTPA (α -methoxy- α -(trifluoromethyl)phenylacetyl) chloride were immediately and separately added to the NMR tubes under a N_2 gas stream. The NMR tubes were shaken carefully to thoroughly mix the samples with MTPA chloride. The reaction NMR tubes were permitted to stand at room temperature and monitored by ^1H NMR spectroscopy until completion of the reaction after 8 h. ^1H – ^1H COSY was additionally measured to confirm the assignment of the signals.

Acknowledgments

S.S.E. acknowledges the Egyptian Government (Ministry of High Education) for a doctoral scholarship and University of Düsseldorf for a postdoctoral fellowship. P.P., B.S., and M.H.G.K. thank BMBF for financial support.

References and notes

- Rateb, M. E.; Ebel, R. *Nat. Prod. Rep.* **2011**, 28, 290.
- Blunt, J. W.; Copp, B. R.; Munro, M. H. G.; Northcote, P. T.; Prinsep, M. R. *Nat. Prod. Rep.* **2011**, 28, 196.
- Piel, J. *Nat. Prod. Rep.* **2009**, 26, 338.
- Laatsch, H. In *Frontiers in Marine Biotechnology*; Proksch, P., Müller, W. E. G., Eds.; Horizon Bioscience: Norfolk, UK, 2006; pp 225–228.
- Shimizu, Y.; Li, B. In *Frontiers in Marine Biotechnology*; Proksch, P., Müller, W. E. G., Eds.; Horizon Bioscience: Norfolk, UK, 2006; pp 145–174.
- Gao, S.-S.; Li, X.-M.; Zhang, Y.; Li, C.-S.; Cui, C.-M.; Wang, B.-G. *J. Nat. Prod.* **2011**, 74, 256.
- Debbab, A.; Aly, A. H.; Lin, W. H.; Proksch, P. *Microbial Biotechnol.* **2010**, 3, 544.
- Li, D.-L.; Li, X.-M.; Proksch, P.; Wang, B.-G. *Nat. Prod. Commun.* **2010**, 5, 1583.
- Cui, C.-M.; Li, X.-M.; Li, C.-S.; Proksch, P.; Wang, B.-G. *J. Nat. Prod.* **2010**, 73, 729.
- Trisuwan, K.; Khamthong, N.; Rukachaisirikul, V.; Phongpaichit, S.; Preedanon, S.; Sakayaroj, J. *J. Nat. Prod.* **2010**, 73, 1507.
- Pan, J.-H.; Deng, J.-J.; Chen, Y.-G.; Gao, J.-P.; Lin, Y.-C.; She, Z.-G.; Gu, Y.-C. *Helv. Chim. Acta* **2010**, 93, 1369.
- Wu, Q.-X.; Crews, M. S.; Draskovic, M.; Sohn, J.; Johnson, T. A.; Tenney, K.; Valeriote, F. A.; Yao, X.-J.; Bjeldanes, L. F.; Crews, P. *Org. Lett.* **2010**, 12, 4458.
- Xu, J.; Kjer, J.; Sendker, J.; Wray, V.; Guan, H.; Edrada-Ebel, R.; Müller, W. E. G.; Bayer, M.; Lin, W.; Wu, J.; Proksch, P. *Bioorg. Med. Chem.* **2009**, 17, 7362.
- Lu, Z.; Wang, Y.; Miao, C.; Liu, P.; Hong, K.; Zhu, W. *J. Nat. Prod.* **2009**, 72, 1761.
- Liu, H.; Edrada-Ebel, R.; Ebel, R.; Wang, Y.; Schulz, B.; Draeger, S.; Müller, W. E. G.; Wray, V.; Lin, W.; Proksch, P. *J. Nat. Prod.* **2009**, 72, 1585.
- Xu, J.; Kjer, J.; Sendker, J.; Wray, V.; Guan, H.; Edrada-Ebel, R.; Lin, W.; Wu, J.; Proksch, P. *J. Nat. Prod.* **2009**, 72, 662.
- Li, D.-L.; Li, X.-M.; Li, T.-G.; Dang, H.-Y.; Proksch, P.; Wang, B.-G. *Chem. Pharm. Bull.* **2008**, 56, 1282.
- Proksch, P.; Ebel, R.; Edrada-Ebel, R.; Riebe, F.; Liu, H.; Diesel, A.; Bayer, M.; Li, X.; Lin, W.; Grebenyuk, V.; Müller, W. E. G.; Draeger, S.; Zuccaro, A.; Schulz, B. *Bot. Mar.* **2008**, 51, 209.
- Jadulco, R.; Edrada-Ebel, R.; Ebel, R.; Berg, A.; Schaumann, K.; Wray, V.; Steube, K.; Proksch, P. *J. Nat. Prod.* **2004**, 67, 78.

20. Hiort, J.; Maksimenka, K.; Reichert, M.; Perović-Ottstadt, S.; Lin, W.; Wray, V.; Steube, K.; Schaumann, K.; Weber, H.; Proksch, P.; Ebel, R.; Müller, W. E. G.; Bringmann, G. *J. Nat. Prod.* **2004**, 67, 1532.
21. Lin, W.; Brauers, G.; Ebel, R.; Wray, V.; Berg, A.; Sudarsono; Proksch, P. *J. Nat. Prod.* **2003**, 66, 57.
22. Edrada-Ebel, R.; Heubes, M.; Brauers, G.; Wray, V.; Berg, A.; Gräfe, U.; Wohlfarth, M.; Mühlbacher, J.; Schaumann, K.; Sudarsono; Bringmann, G.; Proksch, P. *J. Nat. Prod.* **2002**, 65, 1598.
23. Wang, C.-Y.; Wang, B.-G.; Brauers, G.; Guan, H.-S.; Proksch, P.; Ebel, R. *J. Nat. Prod.* **2002**, 65, 772.
24. Jadulco, R.; Brauers, G.; Edrada-Ebel, R.; Ebel, R.; Wray, V.; Sudarsono; Proksch, P. *J. Nat. Prod.* **2002**, 65, 730.
25. Brauers, G.; Ebel, R.; Edrada-Ebel, R.; Wray, V.; Berg, A.; Gräfe, U.; Proksch, P. *J. Nat. Prod.* **2001**, 64, 651.
26. Jadulco, R.; Proksch, P.; Wray, V.; Sudarsono; Berg, A.; Gräfe, U. *J. Nat. Prod.* **2001**, 64, 527.
27. Brauers, G.; Edrada-Ebel, R.; Ebel, R.; Proksch, P.; Wray, V.; Berg, A.; Gräfe, U.; Schächtele, C.; Totzke, F.; Finkenzeller, G.; Marme, D.; Kraus, J.; Münchbach, M.; Michel, M.; Bringmann, G.; Schaumann, K. *J. Nat. Prod.* **2000**, 63, 739.
28. Höller, U.; Wright, A. D.; Matthée, G. F.; König, G. M.; Draeger, S.; Aust, H.-J.; Schulz, B. *Mycol. Res.* **2000**, 104, 1354.
29. Qian-Cutrone, J.; Gao, Q.; Huang, S.; Kloor, S. E.; Veitch, J. A.; Shu, Y.-Z. *J. Nat. Prod.* **1994**, 57, 1656.
30. Vijayakumar, E. K. S.; Roy, K.; Chatterjee, S.; Deshmukh, S. K.; Ganguli, B. N.; Fehlhaber, H.-W.; Kogler, H. *J. Org. Chem.* **1996**, 61, 6591.
31. Oka, M.; Iimura, S.; Tenmyo, O.; Sawada, Y.; Sugawara, M.; Ohkusa, N.; Yamamoto, H.; Kawano, K.; Hu, S.-L.; Fukagawa, Y.; Oki, T. *J. Antibiot.* **1993**, 46, 367.
32. Ondeyka, J. G.; Ball, R. G.; Garcia, M. L.; Dombrowski, A. W.; Sabnis, G.; Kaczorowski, G. J.; Zink, D. L.; Bills, G. F.; Goetz, M. A.; Schmalhofer, W. A.; Singh, S. B. *Bioorg. Med. Chem. Lett.* **1995**, 5, 733.
33. Abdel-Lateff, A.; Klemke, C.; König, G. M.; Wright, A. D. *J. Nat. Prod.* **2003**, 66, 706.
34. Alfatafta, A. A.; Gloer, J. B.; Scott, J. A.; Malloch, D. *J. Nat. Prod.* **1994**, 57, 1696.
35. Kohno, J.; Koguchi, Y.; Nishio, M.; Nakao, K.; Kuroda, M.; Shimizu, R.; Ohnuki, T.; Komatsubara, S. *J. Org. Chem.* **2000**, 65, 990.
36. Klemke, C.; Kehraus, S.; Wright, A. D.; König, G. M. *J. Nat. Prod.* **2004**, 67, 1058.
37. Whyte, A. C.; Gloer, J. B.; Scott, J. A.; Malloch, D. *J. Nat. Prod.* **1996**, 59, 765.
38. Kashiwada, Y.; Nonaka, G.-I.; Nishioka, I. *Chem. Pharm. Bull.* **1984**, 32, 3493.
39. Gunasekera, S. P.; Cordell, G. A.; Farnsworth, N. R. *J. Nat. Prod.* **1979**, 42, 658.
40. Hsu, Y.-H.; Nakagawa, M.; Hirota, A.; Shima, S.; Nakayama, M. *Agric. Biol. Chem.* **1988**, 52, 1305.
41. Hsu, Y.-H.; Hirota, A.; Shima, S.; Nakagawa, M.; Nozaki, H.; Tada, T.; Nakayama, M. *Agric. Biol. Chem.* **1987**, 51, 3455.
42. Su, B.-N.; Park, E. J.; Mbawambo, Z. H.; Santarsiero, B. D.; Mesecar, A. D.; Fong, H. H. S.; Pezzuto, J. M.; Kinghorn, A. D. *J. Nat. Prod.* **2002**, 65, 1278.
43. Ellis, M. B. *Dematiaceous hyphomycetes*; Commonwealth Mycological Institute: Kew, Great Britain, 1971. pp 565–575.
44. Ashour, M.; Edrada-Ebel, R.; Ebel, R.; Wray, V.; Wätjen, W.; Padmakumar, K.; Müller, W. E. G.; Lin, W. H.; Proksch, P. *J. Nat. Prod.* **2006**, 69, 1547.
45. Mueller, H.; Kassack, M. U.; Wiese, M. *J. Biomol. Screen.* **2004**, 9, 506.
46. Aly, A. H.; Edrada-Ebel, R.; Indriani, I. D.; Wray, V.; Müller, W. E. G.; Totzke, F.; Zirrgiebel, U.; Schächtele, C.; Kubbutat, M. H. G.; Lin, W. H.; Proksch, P.; Ebel, R. *J. Nat. Prod.* **2008**, 71, 972.
47. Korff, T.; Augustin, H. G. *J. Cell Sci.* **1999**, 112, 3249.
48. Korff, T.; Augustin, H. G. *J. Cell Biol.* **1998**, 143, 1341.